

# Terahertz quantum cascade laser as local oscillator in a heterodyne receiver

H.-W. Hübers, S. G. Pavlov, and A. D. Semenov

German Aerospace Center (DLR)  
Rutherfordstr. 2, 12489 Berlin, Germany  
[heinz-wilhelm.huebers@dlr.de](mailto:heinz-wilhelm.huebers@dlr.de)

R. Köhler, L. Mahler, and A. Tredicucci

NEST-INFM and Scuola Normale Superiore  
Piazza dei Cavalieri 7, 56126 Pisa, Italy

H. E. Beere and D. A. Ritchie

Cavendish Laboratory, University of Cambridge, Madingley Road,  
Cambridge CB3 0HE, United Kingdom

E. H. Linfield

School of Electronic and Electrical Engineering, University of Leeds  
Leeds LS2 9JT, United Kingdom

**Abstract:** Terahertz quantum cascade lasers have been investigated with respect to their performance as a local oscillator in a heterodyne receiver. The beam profile has been measured and transformed in to a close to Gaussian profile resulting in a good matching between the field patterns of the quantum cascade laser and the antenna of a superconducting hot electron bolometric mixer. Noise temperature measurements with the hot electron bolometer and a 2.5 THz quantum cascade laser yielded the same result as with a gas laser as local oscillator.

©2005 Optical Society of America

**OCIS codes:** (140.3070) Infrared and far-infrared lasers; (140.3300) Laser beam shaping; (140.5960) Semiconductor lasers; (300.6310) Spectroscopy, heterodyne.

---

## References and links

1. T. de Graauw and F. P. Helmich, "Herschel-HIFI: the heterodyne instrument for the far-infrared", in *The Promise of the Herschel Space Observatory*, G.L.Pilbratt, J.Cernicharo, A.M.Heras, T.Prusti, R.Harris, eds., Proc. ESA **SP-460**, 45-51 (2001).
2. R. Güsten, I. Camara, P. Hartogh, H.-W. Hübers, U. U. Graf, K. Jacobs, C. Kasemann, H.-P. Röser, R. T. Schieder, G. Schneider, O. Siebertz, J. Stutzki, G. Villanueva, A. Wagner, P. Van der Wal, and A. Wunsch, "GREAT: the German receiver for astronomy at terahertz frequencies," in *Airborne Telescope Systems II*, R. K. Melugin and H. P. Röser, eds., Proc. SPIE **4857**, 56-61 (2002).
3. M. L. Edgar and J. Zmuidzinas, "CASIMIR: a submillimeter heterodyne spectrometer for SOFIA", in *Airborne Telescope Systems*, R. K. Melugin and H. P. Röser, eds., Proc. SPIE **4014**, 31-42 (2000).
4. H.-W. Hübers, A. Semenov, H. Richter, M. Schwarz, B. Günther, K. Smirnov, G. Gol'tsman, and B. Voronov, "Heterodyne Receiver for 3-5 THz with Hot Electron Bolometric Mixer", in: *Millimeter and Submillimeter Detectors for Astronomy II*, J. Zmuidzinas, W. S. Holland, and S. Withington, eds., Proc. SPIE **5498**, 579-586 (2004).
5. R. W. Hoogeveen, P. A. Yagoubov, A. Maurellis, V. P. Koshelets, S. V. Shitov, U. Mair, M. Krocka, G. Wagner, M. Birk, H.-W. Hübers, H. Richter, A. Semenov, G. N. Gol'tsman, B. M. Voronov, B. N. Ellison, B. J. Kerridge, D. N. Matheson, B. Alderman, M. Harman, R. Siddans, and J. Reburn, "New cryogenic heterodyne techniques applied in TELIS: the balloon-borne THz and submillimeter limb sounder for atmospheric research", in *Infrared Spaceborne Remote Sensing XI*, M. Strojnik, ed., Proc. SPIE **5152**, 347-355 (2004).
6. I. Mehdi, "THz local oscillator technology", in *Millimeter and Submillimeter Detectors for Astronomy II*, J. Zmuidzinas, W. S. Holland, and S. Withington, eds., Proc. SPIE **5498**, 103-112 (2004).

7. R. Köhler, A. Tredicucci, F. Beltram, H. E. Beere, E. H. Linfield, A. G. Davies, D. A. Ritchie, R. C. Iotti, F. Rossi, "Terahertz semiconductor-heterostructure laser", *Nature* **417**, 156-159 (2002).
8. B. S. Williams, S. Kumar, Q. Hu, and J. L. Reno, "Operation of terahertz quantum-cascade lasers at 164 K in pulsed mode and at 117 K in continuous-wave mode", *Opt. Express* **13**, 3331-3339 (2005), <http://www.opticsexpress.org/abstract.cfm?URI=OPEX-13-9-3331>.
9. S. Barbieri, J. Alton, H. E. Beere, J. Fowler, E. H. Linfield, and D. A. Ritchie, "2.9 THz quantum cascade lasers operating up to 70 K in continuous wave", *Appl. Phys. Lett.* **85**, 1674-1676 (2004).
10. L. Ajili, G. Scalari, J. Faist, H. E. Beere, J. Fowler, E. H. Linfield, D. A. Ritchie, and A. G. Davies, "High power quantum cascade lasers operating at  $\lambda \approx 87 \mu\text{m}$  and  $130 \mu\text{m}$ ", *Appl. Phys. Lett.* **85**, 3986-3988 (2004).
11. A. Tredicucci, L. Mahler, T. Losco, J. Xu, C. Mauro, R. Köhler, H. E. Beere, D. A. Ritchie, and E. H. Linfield, "Advances in THz quantum cascade lasers: fulfilling the application potential", in *Novel In-Plane Semiconductor Lasers IV*, C. Mermelstein, D. P. Bour, eds., *Proc. SPIE* **5738**, 146-158 (2005).
12. L. Mahler, R. Köhler, A. Tredicucci, F. Beltram, H. E. Beere, E. H. Linfield, D. A. Ritchie, and A. G. Davies, "Single-mode operation of terahertz quantum cascade lasers with distributed feedback resonators", *Appl. Phys. Lett.* **84**, 5446-5448 (2004).
13. A. Barkan, F. K. Tittel, D. M. Mittleman, R. Dengler, P. H. Siegel, G. Scalari, L. Ajili, J. Faist, H. E. Beere, E. H. Linfield, A. G. Davies, and D. A. Ritchie, "Linewidth and tuning characteristics of terahertz quantum cascade lasers", *Opt. Lett.* **29**, 575-577 (2004).
14. C. K. Walker, C. E. Groppi, C. Drouet d'Aubigny, C. Kulesa, A. Hedden, D. Prober, I. Siddiqi, J. Kooi, G. Chen, and A. W. Lichtenberger, "Integrated heterodyne array receivers for submillimeter astronomy", in *Millimeter and Submillimeter Detectors for Astronomy*, T. G. Phillips and J. Zmuidzinas, eds., *Proc. SPIE* **4855**, 349-354 (2002).
15. U. U. Graf and S. Heyminck, "Fourier gratings as submillimeter beam splitters", *IEEE Trans. on Antennas and Propagation* **49**, 542-546 (2001).
16. J. R. Gao, J. N. Hovenier, Z. Q. Yang, J. J. A. Baselmans, A. Baryshew, M. Hajenius, T. M. Klapwijk, A. J. L. Adam, T. O. Klaassen, B. S. Williams, S. Kumar, Q. Hu, and J. L. Reno, "Terahertz heterodyne receiver based on a quantum cascade laser and a superconducting bolometer", *Appl. Phys. Lett.* **86**, 244104 (2005).
17. J. Faist, M. Beck, T. Aellen, and E. Gini, "Quantum-cascade lasers based on a bound-to-continuum transition", *Appl. Phys. Lett.* **78**, 147-149 (2001).
18. L. Mahler, A. Tredicucci, R. Köhler, F. Beltram, H. E. Beere, E. H. Linfield, and D. A. Ritchie, "High performance operation of single-mode terahertz quantum cascade lasers with surface plasmon gratings", submitted to *Appl. Phys. Lett.* (2005).
19. H. P. Röser, H.-W. Hübers, T. W. Crowe, and W. C. B. Peatman, "Nanostructure GaAs Schottky diodes for far-infrared heterodyne receivers", *Infrared Phys. Technol.* **35**, 451-462 (1994).
20. A. D. Semenov, H.-W. Hübers, J. Schubert, G. N. Gol'tsman, A. I. Elantiev, B. M. Voronov, and E. M. Gershenzon, "Design and performance of the lattice-cooled hot-electron terahertz mixer", *J. Appl. Phys.* **88**, 6758-6767 (2000).
21. H.-W. Hübers, J. Schubert, A. Krabbe, M. Birk, G. Wagner, A. Semenov, G. Gol'tsman, B. Voronov, and E. M. Gershenzon, "Parylene anti-reflection coating of a quasi-optical hot-electron bolometric mixer at terahertz frequencies", *Infrared Phys. and Technol.* **42**, 41-47 (2001).
22. H. Ekström, B. S. Karasik, E. L. Kollberg, and K. S. Yngvesson, "Conversion gain and noise of niobium superconducting hot-electron mixers", *IEEE Trans. Microwave Theory and Tech.* **43**, 938-947 (1995).

---

## 1. Introduction

High resolution heterodyne spectroscopy of molecular rotational lines and fine structure lines of atoms or ions is a powerful tool for exploring the interstellar medium as well as planetary atmospheres including Earth. The terahertz (THz) part of the electromagnetic spectrum is especially rich in these lines. Some examples are the CII fine structure line at 1.6 THz, the OH rotational transitions at 1.8 THz, 2.5 THz, and 3.5 THz, and the OI fine structure line at 4.7 THz. Several upcoming missions are equipped with heterodyne receivers working above 1 THz. The heterodyne instrument for the far-infrared (HIFI) on the Herschel satellite will operate up to 1.9 THz [1]. SOFIA, the Stratospheric Observatory for Infrared Astronomy, will be equipped with two heterodyne receivers covering several frequency bands up to 4.7 THz [2-4], and TELIS, the THz and sub-mm limb sounder, has a frequency channel at 1.8 THz in order to measure OH in the atmosphere of Earth [5].

Typically, below  $\sim 2$  THz multiplied microwave sources are used as a local oscillator (LO). State of the art sources deliver as much as  $40 \mu\text{W}$  power [6]. However, at higher frequencies, the output power is still too low. Above  $\sim 2$  THz optically pumped gas lasers are used. They are relatively bulky and, more importantly, not tunable in frequency [4]. Recently developed THz quantum cascade lasers (QCL) are a promising alternative [7]. The lasing mechanism is

based on intersubband transitions in the conduction band of GaAs/AlGaAs heterostructures. Attractive features, which have been demonstrated so far, are laser emission between 1.9 THz and 4.8 THz, operation temperatures up to ~160 K, high output power up to ~90 mW, single mode operation and narrow linewidth [8-13]. In addition, the frequency of the QCL can be tuned by changing the operation temperature or the current. While this yields a relatively small range of tunability, an external resonator can allow tuning of the QCL frequency across the whole gain profile.

Although QCLs have large output power compared to multiplied microwave sources, pumping of a mixer such as a hot electron bolometer (HEB) might not be a straightforward task since the beam of the QCL has to be matched to the beam pattern of the mixer antenna. While for single pixel receivers the coupling efficiency between QCL and mixer does not need to be very high, an array receiver will require a very well shaped LO beam, normally a Gaussian beam profile. For example an array receiver with up to 100 HEB mixers [14] and coupling of LO and signal radiation by a beamsplitter will require a LO with a few mW power. Coupling by a diplexer might reduce this to several 100  $\mu$ W. Another issue is the distribution of power from a single LO to all mixers in the array. This can be done in an elegant way by using reflective phase gratings (Fourier gratings), which allow splitting a single beam into multiple ones [15]. However these gratings require well shaped beams in order to achieve optimum output. In this paper we will report on the characterization of a 2.5 THz and a 4.3 THz QCL with respect to performance parameters which are relevant for a LO. In contrast to a recent study [16] emphasis is placed on the characterization and shaping of the beam profile of the QCL. Finally noise temperature measurements of a HEB mixer with a QCL LO and a gas laser LO will be presented.

## 2. Quantum cascade laser design

The two QCL structures are both based on a GaAs/AlGaAs superlattice and a plasmon-type waveguide. The 4.3 THz laser design is similar to the one described in Ref. [7] with a chirped superlattice consisting of 104 repeat units each containing a 53 nm wide injector and a 52 nm wide active region. A buried 800-nm thick highly doped ( $2 \times 10^{18} \text{ cm}^{-3}$ )  $n^+$ -GaAs layer forms the boundary between the active medium and the undoped GaAs substrate (~250  $\mu$ m thick). A 200-nm thick doped ( $5 \times 10^{18} \text{ cm}^{-3}$ ) GaAs layer and a Cr/Au layer on top of the active region confine the laser mode from this side. The laser is 150  $\mu$ m wide and 3.1 mm long. One of the facets is coated in order to provide a high quality Fabry-Perot cavity. The laser threshold is at 800 mA and the output is a single mode. The 2.5 THz QCL is based on the so-called bound-to-continuum approach [17] with a rather uniformly chirped superlattice and no marked distinction between the injection and lasing regions [18]. The active medium is formed by 110 repeat units of the superlattice (total thickness 15  $\mu$ m) covered on top by a Cr/Au layer. Between the ~250  $\mu$ m thick substrate and the active medium is a highly doped GaAs layer. Contrary to the 4.3 THz laser, this layer has two doping concentrations:  $2.7 \times 10^{18} \text{ cm}^{-3}$  in the 530 nm next to the superlattice and  $2.6 \times 10^{17} \text{ cm}^{-3}$  in the 500 nm close to the substrate. By these means the boundary conditions at the two sides of the buried doped layer can be controlled separately. This laser also has a Fabry-Perot cavity that is 240  $\mu$ m wide and 2.5 mm long. It has a maximum output power of 6 mW and operates up to 58 K in cw mode. More details such as light-current curves can be found in Ref. [18]. Both lasers are soldered to copper bars, wire bonded, and mounted on the cold finger of a mechanical cryo-cooler. The cooler has a heat extraction capacity of 1 W at 4 K. Since the input power of the lasers is 5-10 W the actual temperature at the cold finger is ~12 K during laser operation.

## 3. Beam profiles

The beam profiles of the two above described QCLs have been measured by scanning a Golay cell detector with a 1 mm diameter aperture in a plane orthogonal to the emission direction of the QCL. The beam profiles are displayed in Fig. 1 along with the orientation of the QCL. At 4.3 THz two emission maxima can be distinguished. One is almost circular while the other has

a trapezoidal shape and higher peak power. We attribute the circular shaped emission to the substrate and the trapezoidal one to the active medium. By integrating the signals of the two lobes separately the confinement factor was determined to be 0.49 which is in agreement with the computed value (0.47) [7].

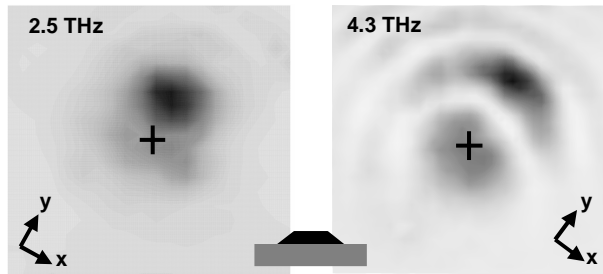


Fig. 1. Beam profiles ( $40 \times 40 \text{ mm}^2$  area) of the 2.5 THz QCL (left panel) and the 4.3 THz QCL (right panel) measured at 61 mm and 77 mm distance, respectively. The inset shows the orientation of the QCL (ridge on top, substrate at the bottom). The cross marks the position of the QCL projected into the beam diagram.

The beam profile of the 2.5 THz QCL differs from the 4.3 THz one. It consists of a slightly elongated emission with a maximum in the upper half and a plateau in the lower half. The peak power is two times higher than the maximum level of the plateau. We attribute the emission of the maximum coming mostly from the laser ridge while the plateau can be attributed to the substrate part. The profiles are somewhat rotated with respect to the orientation of the QCL. This is possibly due to diffraction effects at the laser output facet and the mode in the laser. In the x-direction (for a definition of the direction see Fig. 1) the full width at half maximum (FWHM) is about the same for both lasers for the ridge ( $\sim 7^\circ$ ) as well as for the substrate part ( $\sim 11^\circ$ ), indicating that the divergence is determined by  $\lambda/w$  with  $w$  the width of the ridge, because this ratio is the same for both lasers. In the y-direction the divergence of the laser beam scales with the wavelength. Figure 2 illustrates this: the upper curve a) is a cross section of the 4.3 THz beam profile while the lowest curve c) is a cross section of the 2.5 THz profile. Curve b) is the same as curve a) but the diffraction of the substrate and ridge portions has been scaled from 4.3 THz to 2.5 THz by changing only the wavelength. As can be seen the profiles b) and c) are very similar, indicating that the beam profile is diffraction limited by the same aperture. The fringe pattern of the 4.3 THz laser seen in Figs. 1 and 2 corresponds to a diffracting aperture of  $\sim 280 \mu\text{m}$  assuming plane wave illumination and a refractive index  $n = 3.7$ . This is close to the thickness of substrate and ridge.

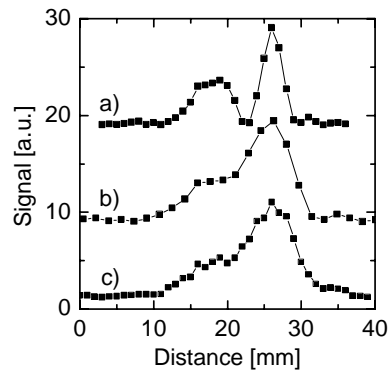


Fig. 2. Cross sections of the beam profiles shown in Fig. 1. a) cross section of the 4.3 THz beam profile, c) cross section of the 2.5 THz profile, b) same cross section as in curve a) but scaled to 2.5 THz. The center of the QCL is at 20 mm.

For use as a LO the beam of the QCL was transformed with a single TPX lens with a focal length of 85 mm in order to match the field pattern of the HEB antenna. The resulting beam profile (Fig. 3) is fairly symmetric (FWHM 1.72 – 1.87 mm). About 60% of the total energy is in the central spot and the first sidelobe is at a level of 10% from the peak value. This is somewhat worse than expected for a circular aperture illuminated by a plane wave. The overlap integral between the main lobe of the QCL profile and a Gaussian beam yields a coupling efficiency of  $\sim 70\%$ . Taking into account the non-Gaussian beam profile of the QCL and some truncation by the TPX lens we consider this as an excellent value.

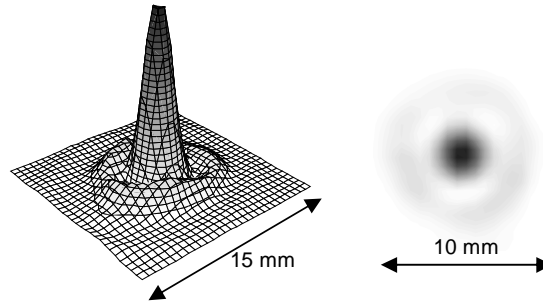


Fig. 3. Beam profile of the QCL at the position of the HEB mixer ( $\sim 800$  mm from the QCL) after passing through a TPX lens (focal length 85 mm).

#### 4. Linewidth

The linewidth of the 2.5 THz QCL was measured by mixing two of its intrinsic modes. The QCL was driven with a current of 870 mA resulting in two longitudinal modes with a separation of  $\sim 15$  GHz. These modes were focused into a GaAs Schottky diode with a quasi-optical  $4\lambda$  corner cube antenna [19]. The signal at the difference frequency was amplified and analyzed with a spectrum analyzer (Fig. 4). A Lorentzian fit to the profile of the difference signal indicates a FWHM of  $\sim 30$  kHz which is comparable with the resolution bandwidth of the spectrum analyzer (30 kHz) and with measurements on another QCL [13]. Assuming that both modes have the same width a single mode is less than  $\sim 20$  kHz wide. The difference signal broadens to several MHz when the acquisition time is increased from 4 ms to 60 s. We attribute this to temperature and current fluctuations in the QCL induced by the mechanical cooler.

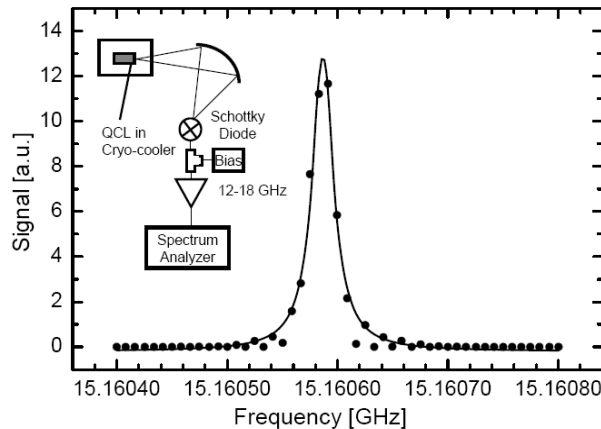


Fig. 4. Difference signal of two longitudinal modes of the 2.5 THz QCL. The FWHM is  $\sim 30$  kHz. This is limited by the bandwidth of the spectrum analyzer (30 kHz). The time for the sweep was 4 ms (inset: experimental set-up).

## 5. Noise temperature measurement

The noise temperature of a phonon-cooled superconducting hot electron bolometer (HEB) was measured with the 2.5 THz QCL acting as LO. The HEB (for more details see Refs. [4, 20]) was a  $2\ \mu\text{m}$  wide,  $0.2\ \mu\text{m}$  long, and  $3.5\ \text{nm}$  thin NbN strip on a high resistivity ( $> 10\ \text{k}\Omega$ ) silicon substrate located in the center of a planar logarithmic spiral antenna. It was glued onto the flat side of an extended hemispherical  $12\ \text{mm}$  diameter silicon lens with a Parylene antireflection coating optimized for  $2.5\ \text{THz}$  [21]. Together they were mounted in a copper holder and put in a liquid helium cryostat equipped with a wedged TPX pressure window and a cold ( $77\ \text{K}$ ) quartz filter. The intermediate frequency (IF) signal was guided out of the mixer via the arms of the antenna and a  $50\ \Omega$  coplanar line. A circulator was used to feed the bias to the mixer and to transmit the IF signal to a  $4\ \text{K}$  low noise HEMT amplifier. The output signal was filtered at  $1.5\ \text{GHz}$  with a bandwidth of  $75\ \text{MHz}$ , further amplified and rectified with a crystal detector. The radiation from the QCL was focused by a TPX lens into the HEB and superimposed with the signal radiation by a  $6\ \mu\text{m}$  thick Mylar beamsplitter. The DSB noise temperature was measured using the Y-factor technique in which a room temperature and a  $77\ \text{K}$  load were alternately placed in the signal path of the mixer (Fig. 5).

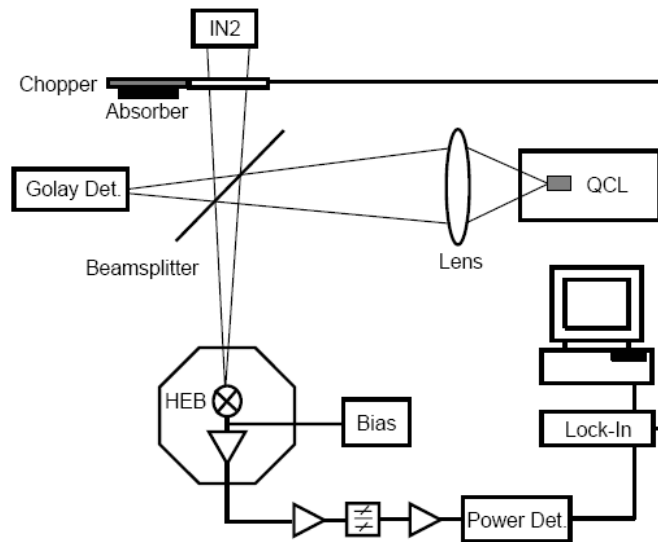


Fig. 5. Experimental set-up for noise temperature measurements with a QCL as LO and a superconducting HEB mixer.

The current-voltage (IV) curves of the HEB as a function of LO power are shown in Fig. 5. The power from the QCL is sufficient to pump the HEB into the normal state (lowest IV curve). In order to achieve the lowest noise temperature the HEB was operated at  $1.3\ \text{mV}/38\ \mu\text{A}$  (square in Fig. 6). This resulted in a double sideband (DSB) noise temperature of  $2700\ \text{K}$ . Even more important than the absolute value is the comparison with the noise temperature achieved with an optically pumped  $2.5\ \text{THz}$  methanol gas laser as LO. With this LO and the same experimental setup except for the TPX lens the same DSB noise temperature as with the QCL was measured. The optimal noise temperature was achieved for  $\sim 10\ \mu\text{W}$  LO power in front of the cryostat window. With the gas laser LO  $\sim 7\ \mu\text{W}$  were required which is somewhat less than with the QCL probably because of the better beam profile. The power inside the superconducting bridge as determined by the isothermal method [22] yields  $\sim 200\ \text{nW}$ . The difference is due to losses in the optical elements and coupling losses between the beam pattern of the HEB antenna and the laser beam profile.

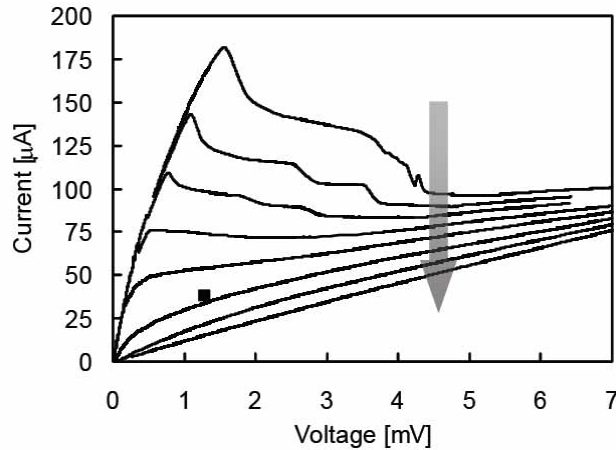


Fig. 6. IV curves of a HEB mixer pumped with a QCL at 2.5 THz. The arrow indicates increasing LO power. The square marks the position where the lowest noise temperature (2700 K DSB) has been obtained. It is worth noting that the same noise temperature has been achieved with a gas laser as LO.

## 6. Summary

In summary, the emission profiles of the investigated QC lasers are asymmetric due to emission originating from the laser ridge and from the substrate. The power ratio between both parts agrees well with the calculated confinement factor. In the growth direction the divergence scales with wavelength whereas perpendicularly it is determined by the ratio of wavelength and width of the ridge. The beam profile can be shaped into a close to Gaussian profile allowing for efficient coupling of the LO radiation into a quasi-optical HEB mixer. The noise temperature of the HEB mixer measured at 2.5 THz with a QCL and a gas laser was the same. The results show that the QCL is very promising device as a LO in an all solid state THz heterodyne receiver.

## Acknowledgement

This work was supported in part by the European Commission through the PASR project "Terasec".